Renewable and Sustainable Energy Reviews 37 (2014) 408–423

Contents lists available at ScienceDirect

Renewable and Sustainable Energy Reviews

journal homepage: www.elsevier.com/locate/rser

Break-even analysis and optimization of a stand-alone hybrid system with battery storage for residential load consumption—A case study

Souheil El Alimi*, Taher Maatallah, Sassi Ben Nasrallah

Energy and Thermal Systems Laboratory, National Engineering School of Monastir, University of Monastir, Avenue Ibn El Jazzar, 5019 Monastir, Tunisia

A R T I C L E I N F O

Article history:
Received 22 August 2013
Received in revised form
13 March 2014
Accepted 27 April 2014
Available online 3 June 2014

Keywords:
Hybrid energy system
Solar PV
Wind
Modeling
Optimization

A B S T R A C T

To assure a real penetration of the enormous intermittent and dispersed naturally renewable resources especially solar and wind, optimal sizing of hybrid renewable power generation systems provide evidence to be indispensable. A determinist technique has been developed to optimize the annual capital cost and the levelized cost of energy of a stand-alone hybrid generation system. Generation and storage units for three systems (wind, photovoltaic, and hybrid photovoltaic–wind turbine) are optimally sized in order to meet the annual load and minimize the capital annualized cost. A case study is conducted to analyze one hybrid project, which is designed to supply residential household located in Monastir city, Tunisia.

Contents

1. Introduction

One of the major challenges confronting users and designers of wind and solar energy systems is the casual, unpredictable nature of the energy sources [1]. In one hand, the photovoltaic (PV) stand-alone system is an expensive option and it depends on the variation of sunshine periods. In the other hand, the stand-alone wind energy conversion system can provide an utilizable energy in a portion of the time during the year due to high cut-in wind speeds which range from 3.5 to 4 m/s [2] and due to the significant fluctuations in the magnitude of wind speeds from 1 h to another throughout the year. Hence, a stand-alone solar energy or wind energy system properly cannot match the electricity demand of consumers due to the high monthly and seasonal variations and

* Corresponding author. Tel.: +216 98 45 20 98; fax: +216 73 50 05 14.
E-mail address: souheil.elalimi@gmail.com (S. El Alimi).

http://dx.doi.org/10.1016/j.rser.2014.04.059

the unattended operation mode for extended periods of time. For example, in the winter seasons, the solar radiation is at its lowest level while the wind speed is usually at its highest level. Moreover, during the nights, solar energy cannot be utilized while the wind energy may be exploited efficiently. Hence, simultaneous utilization of multiple energy resources by combining solar and wind energy conversion systems enhances greatly the certainty of meeting load demands. The combined systems, called also hybrid of energy systems (HES), are becoming more and more attractive and being extensively used for substitution of fossil-produced energy, and eventually to decrease air pollution [2].

In reality, the electrical demand can be random that's why stand-alone HES may suffer from intermittent breakdown, which impacts its supply reliability. This may make the HES unreliable relatively compared to the traditional supplies of electrical energy. Therefore, the use of some energy storage devices seems so necessary to provide a high reliability and avoid gross overdesign of the solar and wind system [3,4]. Another advantage of the HES is the possibility to reduce the required energy storage capacity when one of the optimum combinations of photovoltaic and wind energy is used [5,6]. These devices store the excess of electricity demand and subsequently meet the load demand in shortage of HES. The conventional lead-acid battery is the most general energy storage device at the actual time [7]. Generally storage systems are very expensive and need to be reduced to their minimum possible storage size for a renewable energy system in order to be cost effective [8]. However, a hybrid solar–wind power system improves the overall energy output and reduces energy storage requirements [8].

The output generation of the PV and wind turbines depends on the wind speed and solar radiation variations, that's why the batteries are used to store the surplus energy produced and discharge it when the renewable sources are not available [9]. The converter operates at maximum power point tracking mode to extract the maximum possible energy, regardless of the variation in weather conditions. Various operating strategies can be used, depending on the wind and solar availability and the controller topology. For instance, when solar power is not available at night, wind and battery backup will be used to supply the load demand. Moreover, when the output power generated by the two sources and the stored power in the battery bank are insufficient to meet the load power consumption, DC backup generators can be used to increase the reliability of the system.

For any given load condition, an accurate sizing of PV, wind and battery lead to a successful operation of a hybrid energy system [10].

Hybrid power systems are mainly used in remote and rural locations where the cost of supplying power is high. Besides, the daily load profiles are an important parameter in the hybrid system design, as it characterizes the power demand that must be met by the available renewable sources and backups. As the renewable sources vary throughout the day, the excess power is stored and the batteries will act as auxiliary supply to meet the load demand.

Nevertheless, the hybrid energy system presents some problems due to its increased complexity in comparison with single energy systems. This complexity makes the evaluation of the hybrid energy systems more difficult. The solar radiation and wind speed being highly location dependent, the sizing of such hybrid systems requires comprehensive analysis of these variables for a given site in relation to the system cost for different combinations. Hence, it is very important to determine the levels of the energy resources at which the response achieves its optimum. The optimum design parameters depend on the objective function which could be either at its minimum or a maximum values. In this study, we aim to develop an interesting optimization method for a PV/wind hybrid energy system. The objective function has to depend on PV and wind turbine power output and battery capacity.

2. Inspiration and background

In the past, a several surveys [11,12] were based upon a particular scenario with a definite set of design values yielding the optimum solution. Unfortunately, a lot of last approaches provided the optimum solutions without the aptitude to supply a general appreciation about how the total system cost changes as a function of the parameters design size. Recently, numerous research groups have carried out the optimization of autonomous hybrid energy systems. Borowy and Salameh [13] proposed an algorithm to optimize a photovoltaic-array with a battery bank for a standalone hybrid PV/wind system basing on a long-term hourly solar irradiance and peak load demand data. Later, Borowy and Salameh [14] optimized a PV/wind system combined with a battery bank taking into account the cost of the PV modules and battery units. Markvart [15] constructed a graphic technique to optimize the size of the PV/wind energy system basing on the monthly average solar and wind energy values of the south of England. Bagul et al. [16] used the long term data of wind speed, irradiance and ambient temperature measured every hour during 30 years and the load specifications for a typical New England house. They proposed a technique to determine the optimum relationship between the number of PV panels and the number of required storage batteries for the stand-alone hybrid wind–photovoltaic system, to match a certain loss of power probability. Morgan et al. [17] enhanced the sizing and the optimization of the autonomous renewable energy systems by predicting the battery state of voltage (SOV) rather than its state of charge (SOC). In fact, the simulated algorithm permitted them to forecast the hybrid energy system performance as a function of battery temperature. Celik [18] used the long measured hourly weather data of eight years in order to make a techno-economic investigation and optimization of a PV/wind hybrid energy system basing on 1996 weather data from TyB site of Cardiff, UK. The performance of the HES was evaluated in terms of solar and wind energy fractions, battery storage capacity and system cost. Yang et al. [19] utilized an optimization approach basing on the loss of power supply probability (LPSP) model for a PV/wind hybrid system in order to assess its reliability. Mitchell et al.[1] used a heuristic model, based on seasonal averages of wind, solar and load consumption in order to optimize HES for both grid-connected and stand-alone applications. Their model was able to minimize capacity of batteries and stand-by energy import. Tina and al. developed probabilistic methods which incorporated the irregular nature of the resources and the electrical demand in order to eliminate the requirement for time-series data and evaluate the long-term performance of HES [20]. Ashok [21] suggested a model to minimize the life cycle cost of a hybrid energy system and proposed a general model to find an optimal combination of energy components for a usual rural society. Ekren [22] introduced the response surface methodology as a numerical tool to the size optimization of PV/wind hybrid energy system for a given time-varying hourly load demand that is assumed to be the electricity consumption of the global mobile communications station at Izmir Institute of Technology Campus Area, Urla, Turkey. The achieved simulation was based on the hourly mean solar radiation and wind speed data for the period 2001–2003 registered at the meteorological station of Izmir institute. The Response Surface Methodology, used by Ekren, led to a better understanding of the accurate relationship between input variables such as PV size, wind turbine rotor swept area and battery capacity, and output variables such as the hybrid energy system cost.

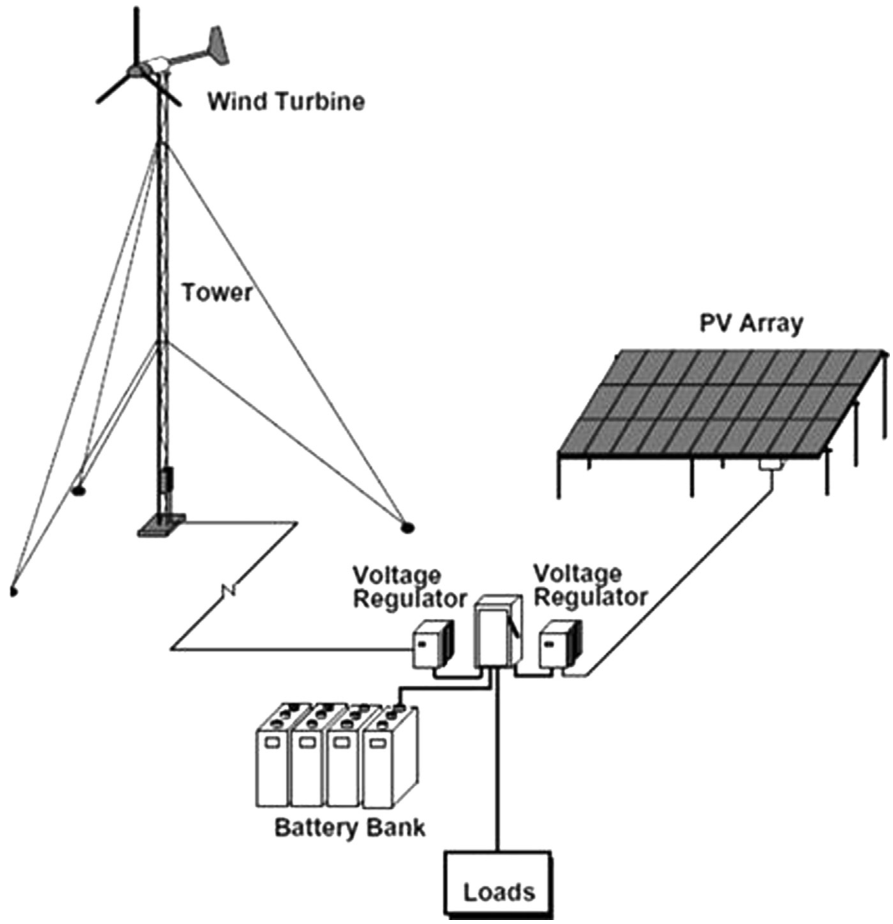


Fig. 1. Typical design of hybrid energy system.

3. Hybrid energy system

The hybrid system relies on solar and wind energies as the primary power resources, and it is backed up by the batteries (see Fig. 1).

Here, batteries are used due to the stochastic characteristics of the system inputs, solar radiation, wind speed and the electricity consumption of the load. The potential energy resources such as solar and wind are not controllable variables and the behavior of these variables are non-deterministic. Therefore, probability distributions are specified in order to carry out a random-input simulation. Hourly solar radiation's and wind speed's theoretical distributions are fitted to a suitable used distribution. In the simulation model, hourly data are used. One of the hybrid system's simulation model assumptions is that the input variables do not change throughout an hour. The length of each simulation run is considered as 20 years of the economic life which consists of 365 days/year, 24 h/day, in total 175,200 h. For each run, five independent replications are completed. In the simulation model, the annualized capital cost C_T is used to compare two or more alternative configurations since it is a popular and useful economical technique [23].

3.1. Solar radiation

The climatic conditions of the Monastir city are favorable for operation in various renewable applications with an annual sunshine hours and an average daily solar radiation received on horizontal plane equal to 2775 h and 4767 kW h/m^2, respectively. We note that the sunshine duration accounts the number of hours for which the measured solar irradiance goes over 120 W/m². The sunshine duration can be expressed other wisely in term of sun cover rate.

Taher et al. [24] recommended that the optimal yearly tilt angle of a fixed solar collector, faced due to the south, in the Monastir city is close to 0.9 times its latitude (33°). Basing on this result, in this study we will use the average hourly solar radiation received on a tilted plane with an inclination of 33° (Fig. 2).

3.2. Wind speed

Monastir city is known by a daily average wind speeds between 4.7 and 7.2 m/s and both stable and high temperatures during the hot and the sunny days. The average hourly wind speed variation gives information about the availability of appropriate winds during the entire 24 h of the day. The hourly wind speed profile which was recorded during the period 1983–2006 is shown in Fig. 3.

3.3. Hybrid energy system modeling

3.3.1. PV model

Knowledge of global solar radiation, using either measured values or estimated ones basing on reliable models, is necessary to PV performance modeling.

3.3.1.1. Global solar radiation

3.3.1.1.1. Beam radiation. The beam radiation on tilted surface, $\overline{G}_{bt}$, can be estimated by multiplying its value received on a horizontal surface, $\overline{G}_b$, by a geometric factor R_b which depends on the zenith and incidence angles. $R_b$is given by the following the expression [25–27]:

$$R_b = \frac{\cos\ \theta}{\cos\ \theta_z} \tag{1}$$

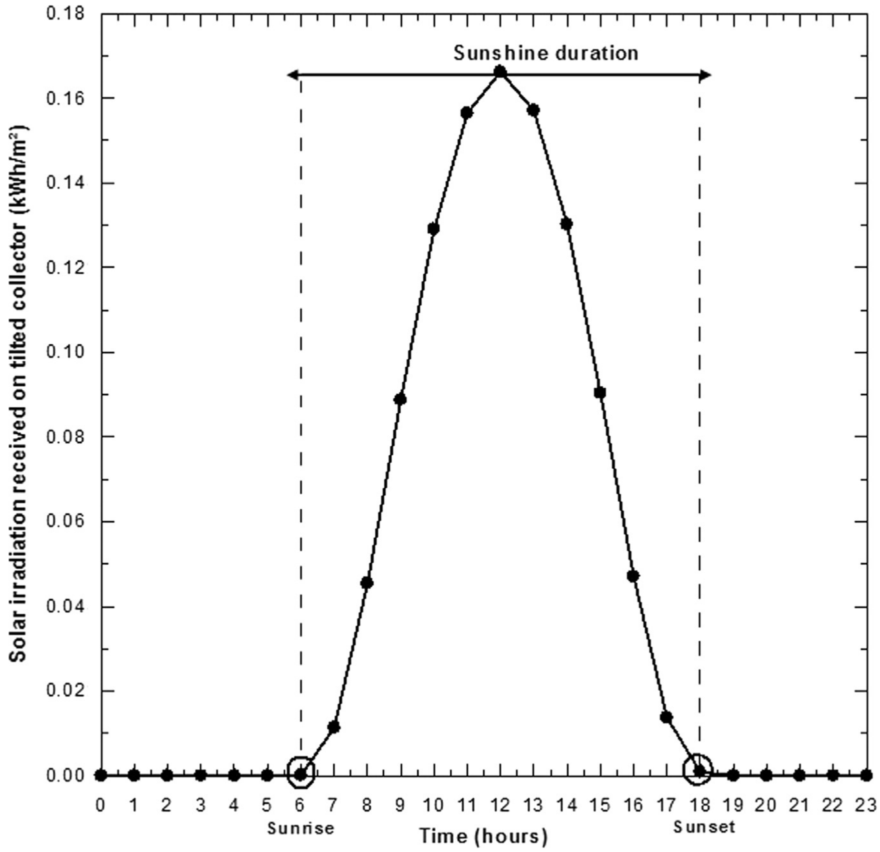


Fig. 2. Average hourly solar radiation of Monastir city received on a tilted solar collector.

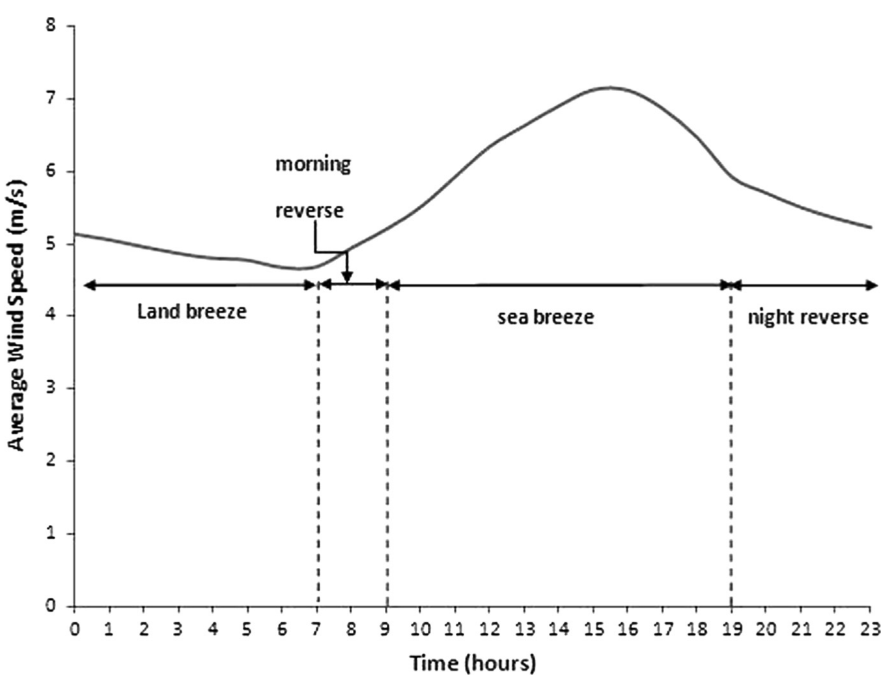


Fig. 3. Long term average wind speed of Monastir city (1983–2006).

Thus, the beam radiation on tilted surface $\overline{G}_{bt}$ is expressed as:

$$\overline{G}_{bt} = \overline{G}_b \times R_b = \overline{G}_b \times \frac{\cos\ \theta}{\cos\ \theta_z} \tag{2}$$

3.3.1.1.2. Diffuse radiation. The diffuse radiation component is the only difference among the models appears in the assessment of the sky-diffuse component [28–33].

It has been pointed out that the sky diffuse component is considered to be the largest potential source of computational

error [34,35]. In fact, the most complex problem of estimating the diffuse irradiance on a tilted surface, $\overline{G}_{dt}$, is related to the fact that it does not have an isotropic distribution in the sky which is not uniform over the time. Many authors investigated the diffuse radiation component basing on various measurements from several stations. In order to evaluate this component, they used various models classified basically on three types: isotropic, circum-solar and anisotropic.

3.3.1.1.3. Isotropic diffuse radiation. The isotropic models presume that the intensity of diffuse radiation is uniform over the entire hemisphere sky dome which could be true in the case of overcast skies. Hence, the diffuse radiation incident on a tilted surface depends on the fraction of the sky dome seen by it [36].

Dorta [37] revealed that many models calculating solar radiation on an tilted surface with any particular orientation have been performed and the isotropic diffuse sky model, Hottel–Woertz–Liu–Jordan [38,39], is the most used. According to this model, the diffuse component can be given as follows:

$$\overline{G}_{dt} = \overline{G}_d \times \left(\frac{1+\cos\beta}{2}\right) \tag{3}$$

where β is the slope of the considered surface.

However, despite the popularity of the isotropic models, theoretical as well as experimental results have shown that the simplified calculations of isotropic model do not give a real picture of the insolation conditions [37]. In fact, they showed the poorest performance and should not be used for estimating the diffuse radiation on a tilted surface [40].

3.3.1.1.4. Circum-solar diffuse radiation. The circum-solar model presumes that all the radiation comes from the direction of the sun and its surroundings, and, therefore, the diffuse component is calculated analogously to the direct component [25]:

$$\overline{G}_{dt} = \overline{G}_d \times R_b \tag{4}$$

Unfortunately, this model could only be applied in the case of completely clear skies, generally overestimates the diffuse component of the radiation [26].

3.3.1.1.5. Anisotropic diffuse radiation. The anisotropic model assume the anisotropy of the diffuse sky radiation in the circumsolar region (sky near the solar disc) and the isotropy diffuse component distribution in the rest of the sky dome. This model is widely accepted, it is used both for clear and cloudy or partly cloudy days [26]. Based on the above, an important number of models considering anisotropic distribution of the diffuse irradiance in the sky are proposed [41–45]. In this context, one of the most confirmed anisotropic sky model is the HDKR, Hay–Davies–Klucher–Reindl, model [37]. This model assumes that there are three components of the diffuse solar radiation: an isotropic component which comes from all parts of the sky equally, a circumsolar diffuse component, which is concentrated in the sky near the sun, and a horizon brightening component which emanates from the sky near the horizon (Fig. 4).

According to The HDKR model, the diffuse component radiation incident on a tilted surface is as follows:

$$\overline{G}_{dt} = \overline{G}_d(R_bA_i) + (1-A_i)\left(\frac{1+\cos\beta}{2}\right)\left[1+f\sin^3\left(\frac{\beta}{2}\right)\right] \tag{5}$$

where f is the factor which accounts the fact that more diffuse radiation comes from the horizon than from the rest of the sky, this modulating correction factor of diffuse radiation includes influence of cloudiness and it is expressed by:

$$f = \sqrt{\frac{\overline{G}_b}{\overline{G}}} \tag{6}$$

A_i is the anisotropy index used to estimate the amount of circumsolar diffuse radiation, also called forward scattered

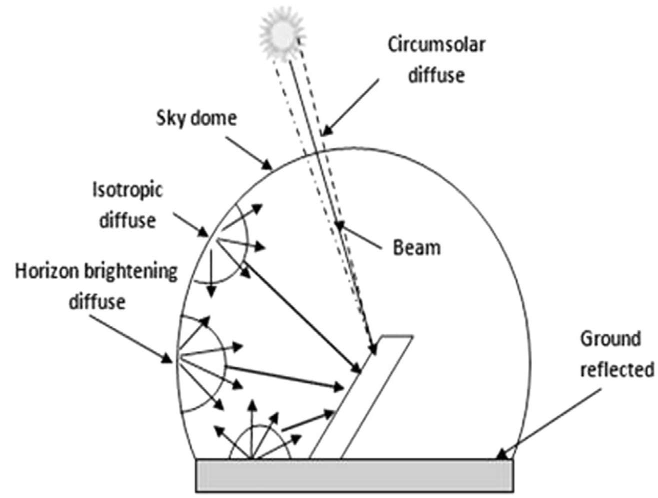


Fig. 4. Schematic view of the solar radiation distribution on a tilted. surface according to anisotropic diffuse sky model.

radiation. This factor is expressed as a ratio of the beam radiation on a horizontal ground surface to the extraterrestrial radiation. Its high value enhances the contribution of circumsolar diffuse radiation. The anisotropy index is given by:

.

$$A_i = \frac{\overline{G}_b}{\overline{G}_o} \tag{7}$$

3.3.1.1.6. Ground reflected radiation. All models assume that the ground reflected component is isotropic and it is expressed as follows [46,47]:

$$\overline{G}_r = \overline{G} \times \rho \times \left(\frac{1-\cos\beta}{2}\right) \tag{8}$$

where ρ is the albedo coefficient of the ground.

3.3.1.1.7. Global radiation. The global radiation on a tilted surface, $\overline{G}_t$, is the sum of the diffuse radiation, $\overline{G}_{dt}$, the beam radiation $\overline{G}_{bt}$, and the ground reflected radiation, $\overline{G}_r$. Therefore, the incident global radiation on tilted surface is given by the following expression [48–53]:

$$\overline{G}_t = \overline{G}_{bt} + \overline{G}_{dt} + \overline{G}_r \tag{9}$$

In this study, the HDKR model will be applied assuming that the global radiation on a tilted surface is given by the following formula:

$$\overline{G}_t = (\overline{G}_b + \overline{G}_dA_i)R_b + \overline{G}_d(1-A_i)R_d\left[1+f\sin^3\left(\frac{\beta}{2}\right)\right] + \overline{G}\rho_gR_r \tag{10}$$

3.3.1.2. PV generation. The PV generation is mainly dependent on the global incident radiation (which was overviewed in the previous section) and the PV cell temperature.

3.3.1.2.1. PV cell temperature. It is well known that the PV cell temperature has an important effect on the PV output power. This temperature can be the same as the ambient temperature during the night but it can go over the ambient temperature by 30° or more in full sun. Hence, it is necessary to calculate the PV cell temperature in order to account for this meaning effect. For this reason, we have to begin by establishing the energy balance between, on one hand, the solar energy absorbed by the PV array, and on the other hand, the electrical output plus the heat transfer to the surroundings. The balance on unit area of the module, which is cooled by losses to the surroundings, can be written as [25]:

$$\tau\alpha G_T = \eta_C\, G_T + U_L(T_C - T_a) \tag{11}$$

where τ, α, G_T, η_C, U_L and T_a are respectively the solar transmittance of the PV array, the solar absorptance of the PV array, the global solar radiation striking the PV module, the electrical conversion efficiency of the PV array, the coefficient of heat transfer to the surroundings and the ambient temperature.

According to The above equation, the PV cell temperature can be expressed as follows:

$$T_C = T_a + G_T\left(\frac{\tau\alpha}{U_L}\right)\left(1-\frac{\eta_C}{\tau\alpha}\right) \quad (12)$$

To estimate the value of $(\tau\alpha/U_L)$, we report the nominal operating cell temperature (NOCT), which is defined as the cell temperature that results at an incident radiation of 0.8 kW/m^2, an ambient temperature of 20 °C, no load operation (meaning $\eta_C = 0$) and an average wind speed equal to 1 m/s [54,55]. We can substitute these values into the above equation and solve it for $(\tau\alpha/U_L)$:

$$\frac{\tau\alpha}{U_L} = \frac{T_{C,\mathrm{NOCT}} - T_{a,\mathrm{NOCT}}}{G_{T,\mathrm{NOCT}}} \quad (13)$$

where $T_{C,\mathrm{NOCT}}$, $T_{a,\mathrm{NOCT}}$ and $G_{T,\mathrm{NOCT}}$ are respectively the nominal operating cell temperature, the ambient temperature and the solar radiation at which the NOCT is defined.

If we presume that $(\tau\alpha/U_L)$ is constant, we can substitute this equation into the cell temperature equation as follows:

$$T_C = T_a + G_T\left(\frac{(T_{C,\mathrm{NOCT}} - T_{a,\mathrm{NOCT}})}{G_{T,\mathrm{NOCT}}}\right)\left(1-\frac{\eta_C}{\tau\alpha}\right) \quad (14)$$

We suppose that the PV array always operates at its maximum power point, which means that the cell efficiency is always equal to the maximum power point efficiency η_{mp}:

$$\eta_C = \eta_{mp} \quad (15)$$

In this order, we can substitute η_C by η_{mp} in the relation (14) which can be written therefore as follows [56]:

$$T_C = T_a + (T_{C,\mathrm{NOCT}} - T_{a,\mathrm{NOCT}})\left(\frac{G_T}{G_{T,\mathrm{NOCT}}}\right)\left(1-\frac{\eta_{mp}}{\tau\alpha}\right) \quad (16)$$

However, η_{mp} depends on the cell temperature T_C, we can assume that the efficiency varies linearly with temperature according to the following equation:

$$\eta_{mp} = \eta_{mp,stc}[1+\alpha_P(T_C - T_{C,stc})] \quad (17)$$

where $\eta_{mp,stc}$, α_P and $T_{C,stc}$ are respectively the maximum power point efficiency under standard test conditions (a radiation of 1 kW/m^2, a cell temperature of 25 °C, and no wind), the temperature coefficient of power and the cell temperature under standard test conditions. We note here that the temperature coefficient of power (α_P) is negative which means that the efficiency of the PV array decreases with increasing cell temperature.

Finally, by substituting this efficiency Eq. (17) into the above cell temperature Eq. (12), the cell temperature becomes:

$$T_C = \frac{T_a + (T_{C,\mathrm{NOCT}} - T_{a,\mathrm{NOCT}})(G_S/G_{S,\mathrm{NOCT}})[1-(\eta_{mp,stc}/\tau\alpha)(1-J\times T_{C,stc})]}{1+(T_{C,\mathrm{NOCT}} - T_{a,\mathrm{NOCT}})(G_S/G_{S,\mathrm{NOCT}})(J\times\eta_{mp,stc}/\tau\alpha)} \quad (18)$$

3.3.1.2.2. PV output power. In this study, we will use one of the simplest models to predict the PV array output power, which assumes that:

$$P_{PV} = Y_{PV} f_{PV}\left(\frac{\overline{G}_T}{\overline{G}_{T,stc}}\right)[1+\alpha_P(T_C - T_{C,stc})] \quad (19)$$

where Y_{PV}, f_{PV}, $\overline{G}_{T,stc}$, α_P, T_C and $T_{C,stc}$ are respectively the rated capacity of the PV array, meaning its power output under standard test conditions, the PV derating factor (it is used to account for such factors as shading, snow cover, aging, and so forth), the incident radiation at standard test conditions, the temperature coefficient of power (which indicates how strongly the PV array power output depends on the cell temperature), the PV cell temperature in the current time step and finally the PV cell temperature under standard test conditions.

3.3.2. Wind model

3.3.2.1. Weibull distribution. The Weibull distribution is often used to characterize wind regimes because it has been found to provide a good fit with measured wind data [57–61]. The probability density function is given as follows [62–69]:

$$f(V) = \frac{K}{C}\left(\frac{V}{C}\right)^{K-1} e^{[-(V/c)^K]} \quad (20)$$

where V, K and C are respectively the wind speed, the shape factor (unitless) and the scale parameter (m/s).

There are several methods which have been proposed to estimate Weibull parameters [70–72]; graphic method, maximum likelihood method and moment method are commonly used to estimate Weibull parameters. Also, a recent method proposed by Akdag and Dinler [73] in 2009 that is referred to "the power density method" will be exhibited in the following section.

Akdag and Dinler [73] have suggested a new method, namely power density method, which is very useful to estimate scale and shape parameters thanks to its easy completion, simple formulation and also needs less computation. Indeed, it does not require binning and solving linear least square problem or iterative procedure.

According to the PD method, the shape parameter, K, can be calculated using the following expression:

$$K = 1 + \frac{3.96}{(E_p)^3} \quad (21)$$

where E_p is the energy pattern which according to the literature is between 1.45 and 4.4 for overall wind distribution in the world [73].

The energy pattern can be expressed also as follows:

$$E_p = \frac{\overline{V^3}}{(\overline{V})^3} \quad (22)$$

where $(\overline{V})^3$ and $\overline{V^3}$ are respectively the average cube of wind speed and the average of wind speed cubes.

After computing the shape parameter using (Eq. (21)), the scale parameter can be also calculated easily using the following expression:

$$c = \frac{\overline{V}}{\Gamma(1+(1/K))} \quad (23)$$

where $\overline{V}$, Γ are respectively the mean wind speed and the gamma function.

3.3.2.2. Energy and power in the wind. The kinetic energy, E_k, of a mass m of air that moves through a cross section A perpendicular to the wind speed V may be expressed as follows [74]:

$$E_k = \frac{1}{2} m V^2 \quad (24)$$

As the mass of air is the product of the air density ρ and the volume of the air that passes through the area A during the period t. The energy E_k may, therefore, be expressed as follows:

$$E_k = \frac{1}{2}(\rho A V t)V^2 = \frac{1}{2}\rho A V^3\, t \quad (25)$$

It is well known that the power of the wind that flows at speed V through a blade swept area A increases as the cubic of its velocity and is given by [75–77]:

$$P(V) = \frac{1}{2}\rho A V^3 \quad (26)$$

The wind power density, $P_d(\rho, V)$, defined as the power per unit of area perpendicular to the direction from which the wind is blowing. $P_d(\rho, V)$ depends on the air density and wind speed. It is given as follows [78]:

$$P_d(\rho, V) = \frac{1}{2}\rho\, V^3 \quad (27)$$

In the above expression, if ρ is expressed in kg/m^3 and V is expressed in m/s $P_d(\rho, V)$ is obtained in W/m^2. $P_d(\rho, V)q)$, is the basic unit for measuring the power contained in the wind [79].

Wind power density of a site based on a Weibull probability density function can be expressed as follows [80]:

$$\frac{P}{A} = \int_0^\infty P(V) f(V) dV = \frac{1}{2}\rho c^3 \Gamma\left(\frac{k+3}{k}\right) \quad (28)$$

Once wind power density of a site is given, the wind energy density for a desired duration (a month or a year) can be expressed as:

$$\frac{E}{A} = \frac{1}{2}\rho c^3 \Gamma\left(\frac{k+3}{k}\right) T \quad (29)$$

where T is the time period (or duration). For example, T is 720 h for monthly duration.

3.3.2.3. Wind output energy. Basing on Weibull representative data, the output energy, E_{WTR} , is given by [81]:

$$E_{\mathrm{WTR}} = \sum_{i=1}^{N} P_{\mathrm{out},i} \times f(V_i) \times N \times \Delta t_i \quad (30)$$

where $P_{\mathrm{out},i}$, $f(V_i)$, N and Δt_i are respectively the fitted power output of a given wind turbine corresponding to the V_i wind speed, the Weibull frequency distribution of V_i wind speed, the total number of measurement for a particular period of the year and the hourly time interval.

3.3.3. Diesel generator model

The use of diesel generator is common in many hybrid energy systems to guarantee supply continuity and battery charge for energy storage. Experimental studies [21] have been found that for a diesel generator, a linear function fits for light load working conditions, while in proximity of rated power, it asks for quadratic expression. For a given time interval, the rate of fuel F, consumed by the diesel generator delivering the power P, is expressed in general as:

$$F = aP^2 + bP + c \quad (31)$$

Table 1
Design variables used for the studied a hybrid energy system.

Variable	Value
Annual interest rate	6%
Life span of the system	20 years
PV panel cost (Kyocera KD 185 GX-LP)	€437
Solar panel installation fee	50% of the price
Wind turbine cost (Whisper 200)	€4379
Wind turbine installation fee	25% of the price
Unit cost of battery (Enersol 50)	€142
Backup generator cost (BC Electronic)	€ 900
Usage% of battery's rated capacity	80%
Battery's rated capacity	624 W/h
Battery's life span	1500 cycles
Maintenance cost for PV array	€0.005 per kW h
Maintenance cost for wind turbine	€0.02 per kW h

Table 2
Hourly electrical consumption distribution for the different household appliances: case A.

Household appliances	Power (W)	0–1	1–2	2–3	3–4	4–5	5–6	6–7	7–8	8–9	9–10	10–11	11–12	12–13	13–14	14–15	15–16	16–17	17–18	18–19	19–20	20–21	21–22	22–23	23–00
TV in use	100.0								1						1						1	1	1	1	
TV standby	3.0	1	1	1	1	1	1	1		1	1	1	1	1		1	1	1	1	1					1
Fridges	200.0	1	1	1	1	1	1	1	1	1	1	1	1	1	1	1	1	1	1	1	1	1	1	1	1
Mobile phone charger	4.0																					3	3	3	3
Washing machine	2000.0							0.5																	
Broadband modems	4.0	1	1	1	1	1	1	1	1	1	1	1	1	1	1	1	1	1	1	1	1	1	1	1	1
Burglar alarms	5.0	1	1	1	1	1	1	1	1	1	1	1	1	1	1	1	1	1	1	1	1	1	1	1	1
Computer in use	100.0																					1	1		
Computer standby	7.1	1	1	1	1	1	1	1	1	1	1	1	1	1	1	1	1	1	1	1	1			1	1
Lighting (incandescent)	40.0							10												8	8	6	4	4	2
Microwave oven	1000.0								0.1					0.2											
Air-conditioner	2600.0													1	1							1	1	1	
Total load (W)		219.1	219.1	219.1	219.1	219.1	219.1	1619.1	416.1	219.1	219.1	219.1	219.1	3019.1	2916.1	219.1	219.1	219.1	219.1	539.1	636.1	3261.1	3181.1	3088.1	311.1

where a, b and c are the coefficients of diesel generator as obtained from the manufacturers' data.

3.3.4. Battery model

In hybrid energy systems, battery bank is required for storage of intermittent wind and solar energy. The battery state charge can be computed as follows:

Battery charging,

$$P_b(t) = P_b(t-1) \times (1-\sigma) + \left(\frac{P_h(t) - P_l(t)}{\eta_i}\right) \times \eta_b \tag{32}$$

Battery discharging,

$$P_b(t) = P_b(t-1) \times (1-\sigma) + \left(\frac{P_h(t)}{\eta_i} - P_l(t)\right) \tag{33}$$

where $P_b(t-1)$, $P_b(t)$, are respectively the battery energy at the beginning and the end of interval t, $P_l(t)$ and $P_h(t)$ are respectively the load demand and the hybrid energy generated by PV array and wind generators at the time t, σ, η_i and η_b are respectively the self-discharge factor, the inverter efficiency and the battery charging which are specified by the manufacturers' data.

The number of batteries N_{BAT} can be computed using the following expression [82]:

$$N_{\rm BAT}(N_{PV}, N_{WT}) = \text{Roundup}\left[\frac{S_{\rm Req}}{\eta S_{\rm BAT}}\right] \tag{34}$$

where Roundup(.), $S_{\rm Req}$,η and $S_{\rm BAT}$ are respectively the function which returns a number rounded up to an integer number, the required storage capacity; the usage percent of rated capacity which guarantees battery's life span and the rated capacity of each battery. We note that the required storage capacity S_{Req} is a function of number of solar panels N_{PV} and number of wind turbines N_{WT} as follows:

$$S_{\rm Rec}(N_{PV}, N_{WT}) = \sum_{t=1}^{\text{Max } t}(P_{PV}^t + P_{WT}^t - P_{Dmd}^t)\Delta t - \sum_{t=1}^{\text{Min } t}(P_{PV}^t + P_{WT}^t - P_{Dmd}^t)\Delta t \tag{35}$$

where Max$t$ is the time when cumulative energy (kW h) is highest; Mint is the time when cumulative energy (kW h) is lowest; Δt is the unit time step; P_{PV}^t is the output power (kW) generated by the PV panels at time t; P_{WT}^t is the power (kW) generated by wind turbines at time t; and P_{Dmd}^t is the power (kW) demanded at time t. Besides, the PV power generation can be calculated as follows:

$$P_{PV}^t = N_{PV} \times P_{\,PV_Each} \tag{36}$$

where $P_{\,PV_Each}$ is the power (kW) generated by each PV panel at time t. $P_{\,PV_Each}$ can be obtained as it was mentioned in Section 3.3.1.2.1. Also, the power generated by wind turbines can be calculated as follows:

$$P_{WT}^t = N_{WT} \times P_{\,WT_Each} \tag{37}$$

where $P_{\,WT_Each}$ is the power (kW) generated by each wind turbine at time t. $P_{\,WT_Each}$ can be calculated using Section 3.3.2.3.

4. Optimization formulation

The objective function of the hybrid energy system design is the minimization of total design cost C_T which consists of total capital cost C_{cpt} and total maintenance cost C_{MNT} as follows:

$$\text{Minimize } C_T = C_{Cpt} + C_{\rm MNT} \tag{38}$$

We note that while the capital cost occurs in the beginning of a project, the maintenance cost occurs along the project life.

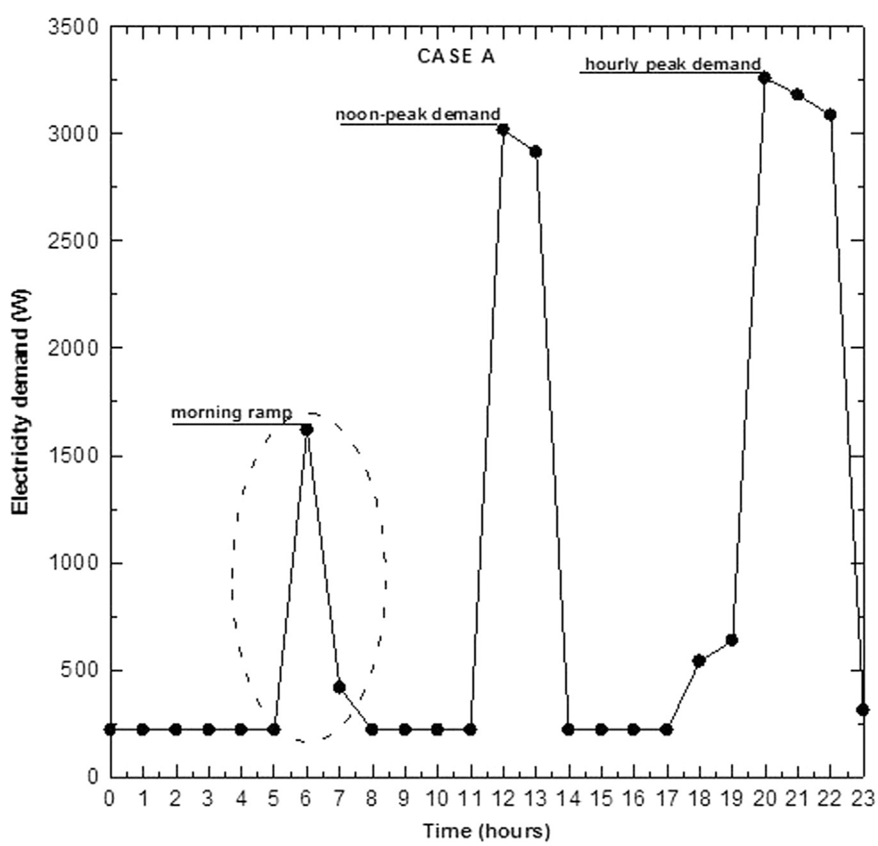


Fig. 5. Hourly profile of the household electricity load (case A).

Table 3
Hourly electrical consumption distribution for the different household appliances: case B.

Household appliances	Power (W)	0–1	1–2	2–3	3–4	4–5	5–6	6–7	7–8	8–9	9–10	10–11	11–12	12–13	13–14	14–15	15–16	16–17	17–18	18–19	19–20	20–21	21–22	22–23	23–00
TV in use	**100.0**																1	1			1	1	1	1	
TV standby	**3.0**	1	1	1	1	1	1	1	1	1	1	1	1	1	1	1			1	1					1
Fridges	**200.0**	1	1	1	1	1	1	1	1	1	1	1	1	1	1	1	1	1	1	1	1	1	1	1	1
Mobile phone charger	**4.0**																					3	3	3	3
Washing machine	**2000.0**																		0.5						
Broadband modems	**4.0**	1	1	1	1	1	1	1	1	1	1	1	1	1	1	1	1	1	1	1	1	1	1	1	1
Burglar alarms	**5.0**	1	1	1	1	1	1	1	1	1	1	1	1	1	1	1	1	1	1	1	1	1	1	1	1
Computer in use	**100.0**																					1	1		
Computer standby	**7.1**	1	1	1	1	1	1	1	1	1	1	1	1	1	1	1	1	1	1	1	1			1	1
Lighting (incandescent)	**40.0**							10												8	8	6	4	4	2
Microwave oven	**1000.0**								0.1							0.2									
Air-conditioner	**2600.0**																1	1				1	1	1	
Total load (W)		**219.1**	**219.1**	**219.1**	**219.1**	**219.1**	**219.1**	**619.1**	**319.1**	**219.1**	**219.1**	**219.1**	**219.1**	**219.1**	**219.1**	**419.1**	**2916.1**	**2916.1**	**1219.1**	**539.1**	**636.1**	**3261.1**	**3181.1**	**3088.1**	**311.1**

Consequently, costs at different times cannot be directly compared, but should first be made equivalent through the use of discount factors that convert a monetary value at one time to an equivalent value at another time [83,84]. For this reason, the initial capital cost P is converted into annual capital cost A using the following capital-recovery factor:

$$\frac{A}{P}=\frac{i(1+i)^n}{(1+i)^n+1} \tag{39}$$

where i and n are respectively the annual interest rate and the life span of the system (in years). Therefore, total annual capital cost C_{Cpt} can be given as follows:

$$C_{Cpt}=\frac{A}{P}\left[N_{PV}C_{PV}+N_{WT}C_{WT}+N_{\text{BAT}}C_{\text{BAT}}+C_{\text{Backup}}\right] \tag{40}$$

where N_{PV} is number of PV panels, C_{PV} is unit cost of PV panel, N_{WT} is number of wind turbines, C_{WT} is unit cost of wind turbine, N_{BAT} is number of batteries, C_{BAT} is unit cost of battery; and C_{Backup} is cost of backup generator for the use when the electricity demand is greater that the PV, wind and stored energies. The unit cost of solar panel C_{PV} consists of panel price and installation fee; and the unit cost of wind turbine C_{WT} consists of turbine price and installation fee.

The total annual maintenance cost C_{MNT} can be expressed as the following:

$$C_{\text{MNT}}=\left[C_{\text{MNT}}^{PV}\times\sum_{t=1}^{24}\left(P_{PV}^{t}\times\Delta t\right)+C_{\text{MNT}}^{WT}\times\sum_{t=1}^{24}\left(P_{WT}^{t}\times\Delta t\right)\right]\times 365 \tag{41}$$

where C_{MNT}^{PV} and C_{MNT}^{WT} are respectively the maintenance cost per kW h for PV array and wind turbine. Here, we have to note that due to the vulnerability of battery in the renewable power generation system, the replacement cost of the battery may be also included in the objective function of the total design cost.

In the optimization problem, several constraints may be imposed. First, the total energy amount generated by the PV panels and wind turbines should be greater than or equal to total energy amount required by users as follows:

$$\sum_{t=1}^{24}\left(P_{PV}^{t}\times\Delta t\right)+\sum_{t=1}^{24}\left(P_{WT}^{t}\times\Delta t\right)\geq\sum_{t=1}^{24}\left(P_{Dmd}^{t}\times\Delta t\right) \tag{42}$$

Second, the numbers of PV panels and wind turbines should be non-negative integer variables as the following:

$$N_{PV}=\text{Integer},\quad N_{PV}\geq 0 \tag{43}$$

$$N_{WT}=\text{Integer},\quad N_{TW}\geq 0 \tag{44}$$

Third, the problem can have optional constraints of resource limitation as follows:

$$N_{PV}\leq N_{PV}^{\max} \tag{45}$$

$$N_{WT}\leq N_{WT}^{\max} \tag{46}$$

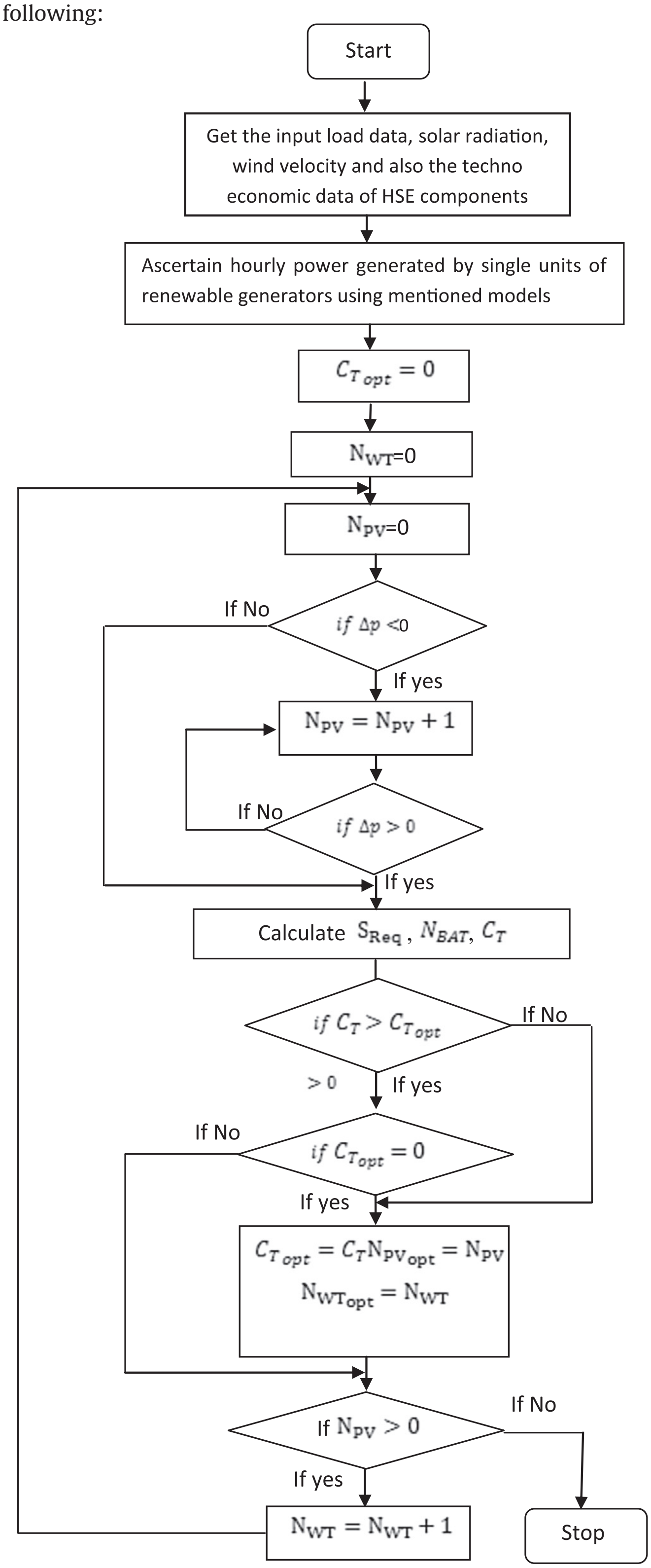
$$N_{BAT}\leq N_{BAT}^{\max} \tag{47}$$

where $N_{PV}^{\max}$, $N_{WT}^{\max}$ and $N_{\text{BAT}}^{\max}$ are respectively the maximum available number of PV panel; the maximum available number of wind turbines and the maximum available number of storage batteries.

Table 1 provides the values of the used design variables. It is noticeable that because the life span of each battery is 4 years, five times of N_{BAT} is required to satisfy the life span of the PV-wind system.

In this paper, a new proposed method was used to solve the optimization problem. This method has a very smart procedure exploration of the parameter space. In fact, this method is relatively simple when comparing with dynamic simulation. It explores all the variable space and records the best element. The objective function C_T is evaluated at a point under the

considered constraints. The new value of C_T is compared to the previous one. If it is better than the previous one, this value is stored as well as the corresponding solution, then the process continues. Otherwise, the process retains the previous point and the procedure continues until stopping conditions are reached. The proposed method draws the region where the solution is acceptable in the parameter space. The flowchart of ascertaining the optimal system configuration in our case study is as the following:



Flowchart of ascertaining the optimal system configuration.

where $\Delta p = (P^t_{PV} + P^t_{WT}) - P^t_{Dmd}$ is the difference between the system output power and the power load consumption for each time step;

- $C_{T\text{opt}}$: optimal actualized total cost of configuration system;
- $N_{PV\text{opt}}$: optimal number of photovoltaic modules;
- $N_{WT\text{opt}}$: optimal number of wind turbines.

The above mentioned optimization technique use mathematical methods to model the PV, wind and battery sources. At the same time, this model depends on availability of weather information and details of manufacturer's data. Indeed, the optimization model requires the following inputs:

– Resources availability (solar radiation data, clearness index and wind velocity) of the site in question for each computational time step;
– Electrical load distribution;
– Technological and economic inputs: all characteristics and prices of components.
– PV module: orientation and tilt angles, optimal output power, thermal power coefficient, temperature of the cells functioning, aging coefficient, module unit cost, installation fee, maintenance cost per kW h and life span.
– Wind turbines: output power curve, hub height, wind turbine unit cost, installation fee, maintenance cost per kW h and life span.
– Battery: nominal capacity, round trip efficiency, float life, unit cost.
– Backup generator: empirical consumption rate coefficients, unit cost, life time.

The proposed optimization algorithm simplifies the task of evaluating system design for variety of combinations. This model simulates the operating of system by making energy balance computations in each time step. In fact, for each time step, this model compares the electrical demand and the output energy that system can supply in that time step, and calculate the flows of energy to and from each component of system under the considered constraints. It then runs for each possible combination of the system (configuration). For configurations that include batteries and backup generators, we also evaluate in each time step how to operate generators and calculate the required storage capacity. The energy calculations for each time system configuration determines whether it is a feasible one; means that whether it can meet the electric demand under the conditions and the constraints that we specify, and it estimates the actualized annual cost system over its lifetime. This system cost calculations account for costs such as capital, replacement, maintenance, installation and interest. After simulating all feasible configurations, only the best annualized cost-effectiveness, which minimizes the objective function C_T, will be stored. We note that we display all optimal configurations of each possible hybrid combination.

5. Outcome results

This section covers the three load consumption distributions, the output power computations of the available resources and the techno-economic deigns of the optimal HES configurations.

5.1. Load consumption

In this study, three cases studies will be considered to define the power consumption of an urban residential building located in the region of Monastir, Tunisia. The latitude and longitude of this town are respectively 36°N and 12°E and an altitude of 10 m above

sea level. We note that this city has a good wind resource and solar deposit that promote the use of renewable energy resources for electricity generation.

For the load consumption, a total of 22,054 W/h is considered as the average daily energy demand for a typical house in the city of Monastir. This average value of a daily energy load was confirmed by a statistical survey which has been established by the Electricity and Gas Tunisian Company (STEG).

Three different distributions are defined, the first one (case A) corresponds to the families who leave their habitats from 8 am, a half-round home at mid-day, another out of the house at 2 pm and the whole family back home at 6 pm. The peak consumption has the values of 416.1, 3019.1 3261.1 W which occurred at 8 pm, noon and 8 am, respectively. Table 2 and Fig. 5 show, respectively, the distribution of the household electrical charge for the different energies equipments and its corresponding hourly profile.

The second profile distribution of the house electricity demand (case B) corresponds to the families who leave their habitats from 8 am and return back at 2 pm. This path can explain the first peak consumption at 6 am with the value of 619 W and during the second half of the day and exactly at 3 pm and 4 pm it reaches a consumption of 2916 W. The last peak of the electricity demand take place during the hours between 8 pm and 10 pm with a maximum of 3261 W. The energy consumption often occurs in the afternoon especially for the needs of air conditioning and in the night for almost imperative lighting and operation of different appliances. Table 3 and Fig. 6 show respectively the distribution of the household electrical charge of the different energy equipments and its corresponding hourly profile.

The third distribution of the power consumption (case C) corresponds to the families which are using for almost of the time their domestic electrical appliances at the night. For this reason, after slight morning peak consumption reached at 6 am having the value of 619 W, the electric charge increases from 6 pm achieving another peak load corresponding to 4261 W at 8 pm. Table 4 and Fig. 7 show respectively the distribution of the household electrical charge of the different energy equipments and its corresponding hourly profile (Table 5).

5.2. Output power resources

Information about the average hourly annual profile of the wind speed and data interpolation of the wind power curve (Whisper 200 W) are very necessary for a confident estimation of the wind turbines efficiency (Fig. 8).

Using the average hourly annual wind speed profile corresponding to the studied region, the interpolated wind power curve of Whisper 200 W and the Weibull model for estimating the wind power (Eq. (15)), we obtain the average hourly annual wind production distribution which is shown in Fig. 9.

Using the HDKR model for estimating global solar radiation and the PV conversion model (Eq. (7)), the average hourly annual PV output power can be shown in Fig. 10.

We note that this study aims mainly to investigate the load profile distribution impact on the optimal hybrid energy configuration. The use of an annual average of solar radiation and wind speed is valid in the North of Africa and especially in Tunisia because this it has quite stable climatic conditions. However, for other locations, especially for higher latitudes where there are extremely high seasonal variation, especially for higher latitudes, it would be interesting to apply the proposed method using an average hourly meteorological data.

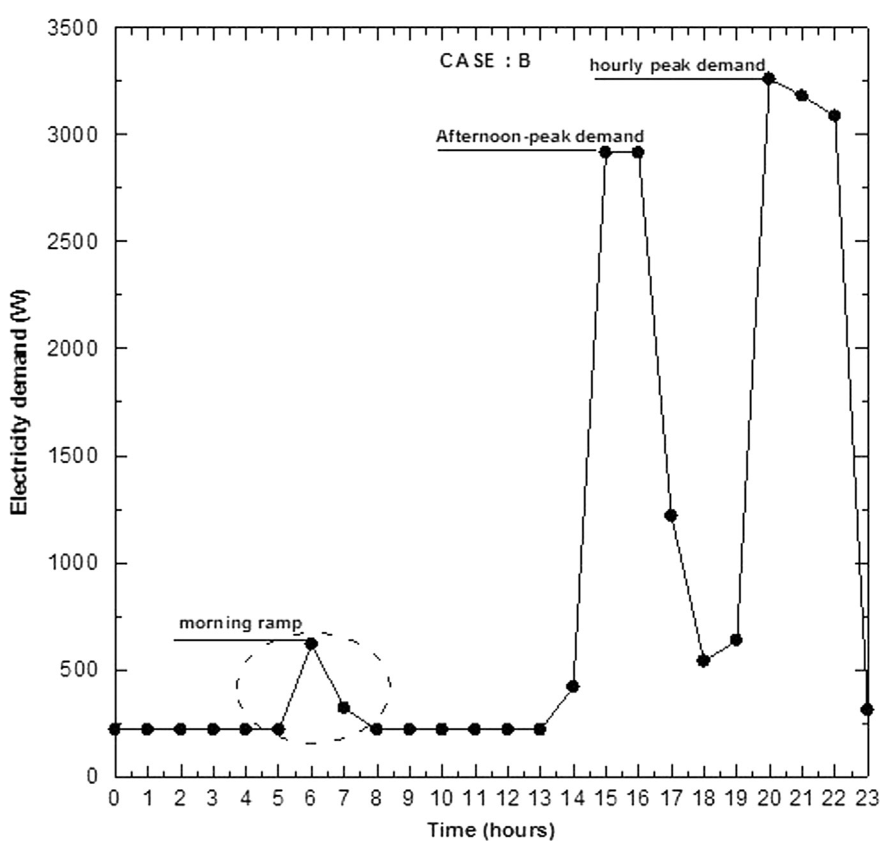


Fig. 6. Hourly profile of the household electricity load (case B).

Table 4
Hourly electrical consumption distribution for the different household appliances: case C.

Household appliances	Power (W)	0–1	1–2	2–3	3–4	4–5	5–6	6–7	7–8	8–9	9–10	10–11	11–12	12–13	13–14	14–15	15–16	16–17	17–18	18–19	19–20	20–21	21–22	22–23	23–00
TV in use	**100.0**																			1	1	1	1	1	1
TV standby	**3.0**	1	1	1	1	1	1	1	1	1	1	1	1	1	1	1	1	1	1						
Fridges	**200.0**	1	1	1	1	1	1	1	1	1	1	1	1	1	1	1	1	1	1	1	1	1	1	1	1
Mobile phone charger	**4.0**																					3	3	3	3
Washing machine	**2000.0**																					0.5			
Broadband modems	**4.0**	1	1	1	1	1	1	1	1	1	1	1	1	1	1	1	1	1	1	1	1	1	1	1	1
Burglar alarms	**5.0**	1	1	1	1	1	1	1	1	1	1	1	1	1	1	1	1	1	1	1	1	1	1	1	1
Computer in use	**100.0**																					1	1		
Computer standby	**7.1**	1	1	1	1	1	1	1	1	1	1	1	1	1	1	1	1	1	1	1	1			1	1
Lighting (incandescent)	**40.0**							10												8	8	6	4	4	2
Microwave oven	**1000.0**								0.1												0.2				
Air-conditioner	**2600.0**														1					1	1	1	1	1	
Total load (W)		**219.1**	**219.1**	**219.1**	**219.1**	**219.1**	**219.1**	**619.1**	**319.1**	**219.1**	**219.1**	**219.1**	**219.1**	**219.1**	**219.1**	**219.1**	**219.1**	**219.1**	**219.1**	**3236.1**	**3436.1**	**4261.1**	**3181.1**	**3088.1**	**408.1**

5.3. Optimal HES configurations

In this simulation, for each case of residential electricity demand set (A, B or C) seven configurations are possible (2^{n-1} where n is the number of available sources in the SEH (PV/Wind/Diesel). For each hour, the developed code simulates all possible combinations. Hour after hour, the load consumption is compared to the available potential energy and the energy flow is adjusted for each system component. Besides, for each hour, we can monitor the functioning of the diesel generator, and the charging and discharging of the batteries bank. As the hybrid system model is introduced with the technological options availability, component costs and resources availability, these inputs are simulated for different combinations of possible components. Hence, Energy balance calculations are performed for each configuration of hybrid system. Profitability operation is assessed on the life of the project which is estimated to 20 years. The used optimization technique is very interesting for combinatorial systems' optimization. Indeed, the technique uses an enumeration of all candidate solutions process ensuring the provision of a global optimum. This method takes the following objective function:

$$\text{Minimize } C_T = \frac{A}{P}\left[N_{PV}C_{PV} + N_{WT}C_{WT} + N_{\text{BAT}}C_{\text{BAT}} + C_{\text{Backup}}\right]$$
$$+\left[C_{\text{MNT}}^{PV} \times \sum_{t=1}^{24}(P_{PV}^{t} \times \Delta t) + C_{\text{MNT}}^{WT} \times \sum_{t=1}^{24}(P_{WT}^{t} \times \Delta t)\right] \times 365$$

The blown table shows the optimal hybrid configuration for each case of distribution for the residential electricity consumption in the region of Monastir. The total annual cost and the levelized cost of energy of each configuration of the hybrid power system are recapitulated in this table. Here, we note that the levelized cost of energy is the constant unit cost (per kW h) of the capital annualized cost of the system over its life. It is clear that for the same average daily energy requirement load, the optimal hybrid energy system is not the same because of the difference in the distribution of peak consumption during the simulation of the three cases of residential load profile.

We note that only the first case (Case A) PV power generation can contribute in the global energy production due to the two electrical peak demands which occur at 6 am and 2 pm. In this case, the presence of 7 PV modules is very effective for both their maximum production coincides with the highest electrical demand. We note also that this configuration is the most cost-effective one with a levelized cost of energy equal to 0.3082 € per kW h over 20 years. Then, we can deduce that the combination (PV/wind) is the best energizing solution because it satisfies, with the minimum annual cost (2481.1023 €), the worst case power distribution in terms of stability. In addition, the optimal configuration of the hybrid energy system in the second case (Case B) does not longer contain the PV solution. This is explained by the fact that periods of high electricity consumption (3–4 pm and 8–10 pm) does not correspond to the maximum PV output power (see Fig. 10), which can lead to quite high operating generators cycles. Hence, the optimal configuration is composed by three wind turbines which their maximum output power fulfill at 3 pm and 4pm (see Fig. 9) and 15 storage batteries. This second optimal configuration generates a cash surplus because the levelized cost of energy is now evaluated to 0.3101 € per kW h. Finally, the third optimal configuration of HES for the third electric charge distribution (case C) retains the same optimal wind design but the number of batteries storage has been increased by 8 ones in comparison relatively with the second case (Case B). This increase of storage

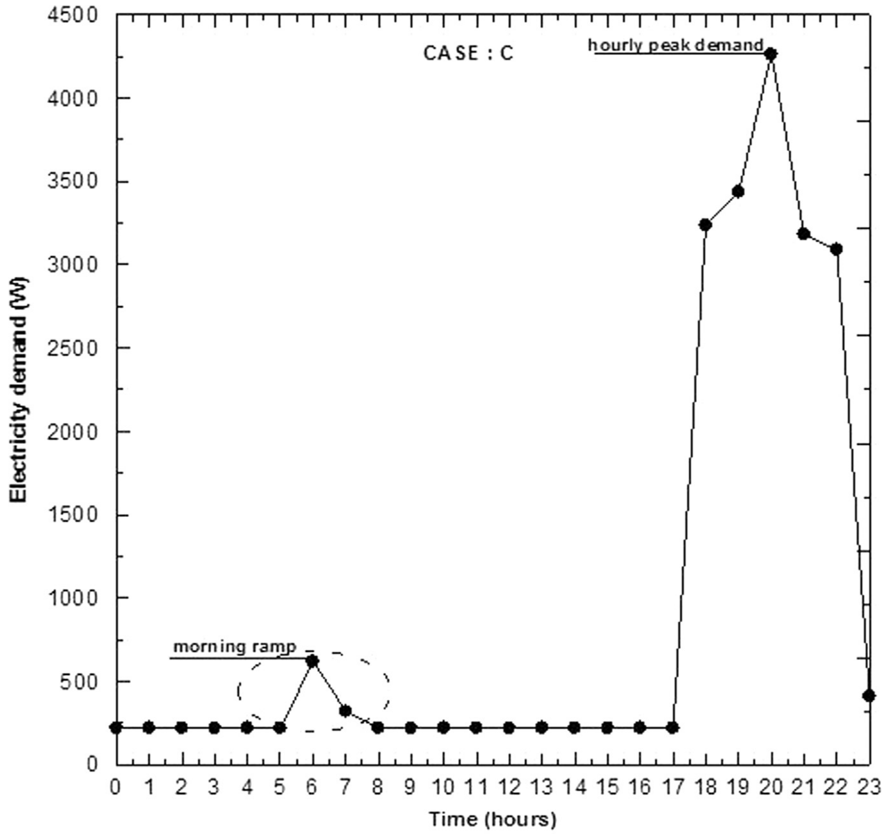


Fig. 7. Hourly profile of the household electricity load (case C).

Table 5
Techno-economic design of each optimal HES configuration.

Load case	Optimal configuration	Annualized total cost C_T (€)	Levelized cost of energy (€/kW h)
Case A	2 WT-7 PVM-15 BS	**2481.1023**	**0.3082**
Case B	3 WT-0 PVM-15 BS	2496.3814	0.3101
Case C	3 WT-0 PVM-23 BS	2991.5896	0.3716

E.I.: WT: Wind Turbine, PVM: Photovoltaic Module and BS: Battery Storage.

capacity is explained by the dominant concentration of electricity demand during the night hours that's why the resulted total annual cost and the levelized cost of energy become higher than the last two cases (which are respectively 0.3716 € per kW h and 2991.5896 €).

The main conclusions drawn from this investigation can be the following:

- The electricity demand distribution is an important factor in the hybrid renewable energy system's optimization and not only the resources availability and the quality of the local renewable deposits.
- The developed optimization model has proved its efficiency in terms of computation time and reliability to achieve the overall optimal configuration without the risk of falling on potential local solutions.
- The HES (PV/wind/diesel) combined with electrochemical storage banks can be a cost-effective energy system and economical solution in medium and long term. The following table recapitulates the optimal hybrid configuration and its total annual cost and the levelized cost of energy of each load demand category.

6. Conclusion

In this study, the sizing of a (PV/Wind/Diesel) hybrid power system with electrochemical storage banks has been optimized using a proposed generic technique based on the principle of the determinist methods. The main objective is to minimize the annual operating cost and the produced Kilowatt of the system over 20 years. First, a complete HES modeling has been developed. Second, the modeling of the supplied electric auxiliary power (diesel generator) and its fuel consumption with the instantaneous state of charge and discharge battery banks has been implemented.

The effectiveness analysis of the SEH was performed in order to decide which investments will be beneficial to cover the energy consumption of standard residential buildings taking into account the non-uniform distribution of the electric charge in the city of Monastir, Tunisia.

An optimization model of the actualized annual cost over the HES life span was made. This optimization model is very useful for the simulation of the medium and the large scale of installed capacity for autonomous renewable systems for. Indeed, this model starts with the optimization design from the optimal energy resources evaluation (estimated solar flux correlations, optimal tilt and azimuth panels, optimal wind speed distribution, optimal interpolated power curves…and so forth) until the development of real relationships between several input variables of the system (number of PV modules, number of wind turbines and storage batteries) and output variables. Then, the results showed that the optimum hybrid system for the same electricity demand depends on

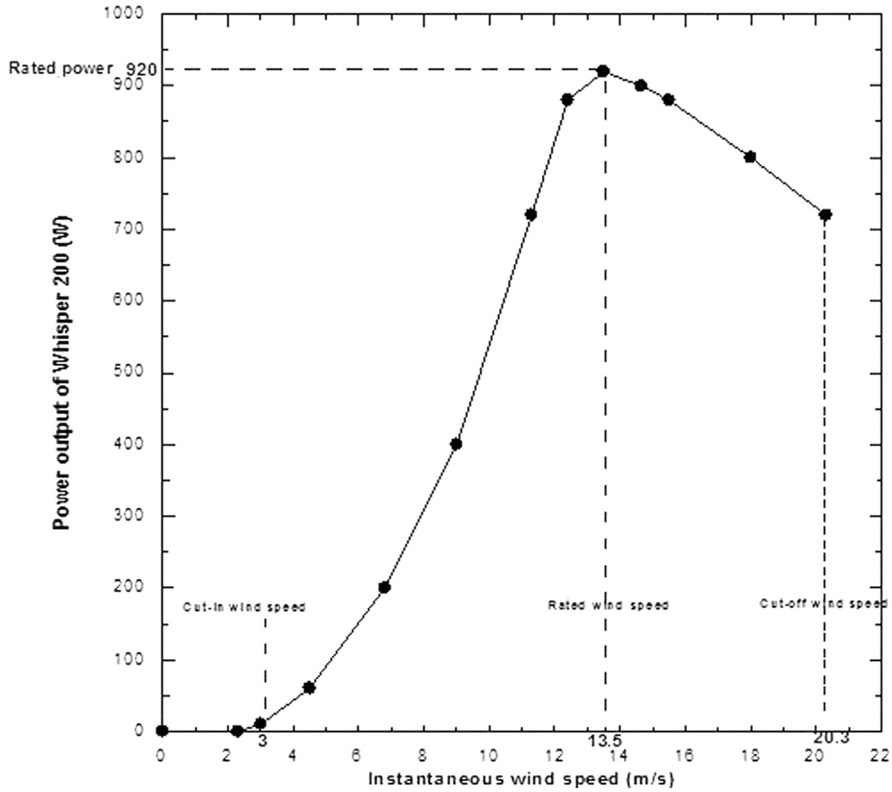


Fig. 8. Power curve of Whisper 200 W.

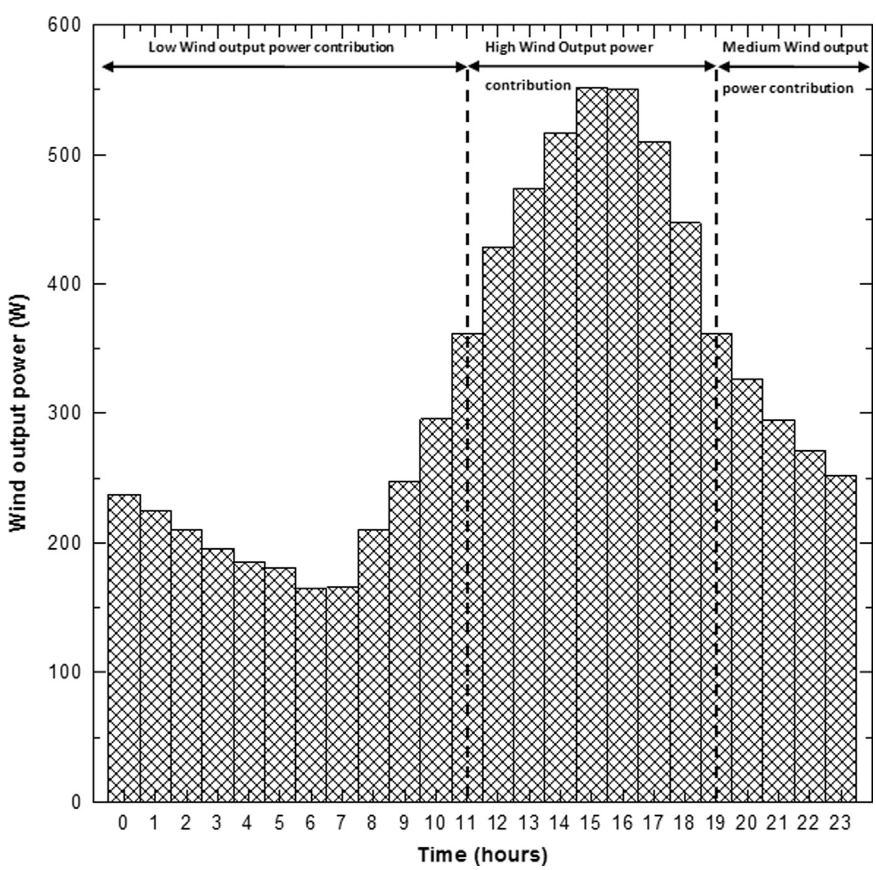


Fig. 9. Hourly output power produced by par wind turbine (Whisper 200 W).

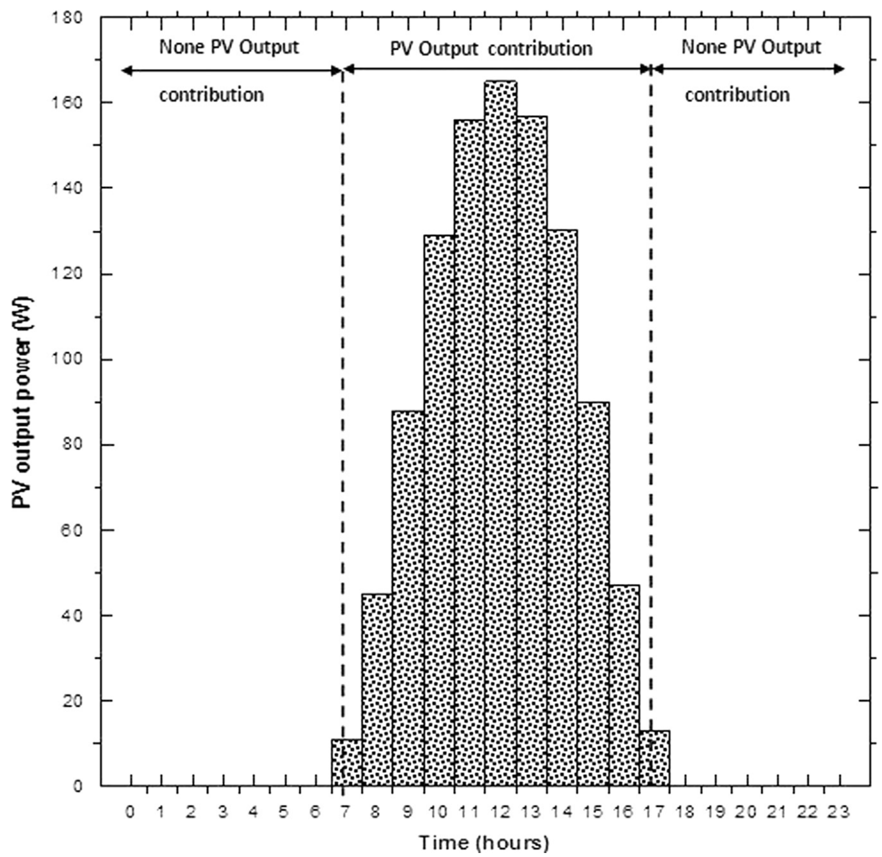


Fig. 10. Hourly output power produced per unit of PV module (Kyocera 185 GK-LP).

the probability distribution of the daily load consumption. The combination (PV/Wind) is the best way to satisfy the most instable electrical demand distribution and in this case the levelized cost of energy does not exceed the value of 0.3082 € per kW h. For electrical applications for which the peak loads occurs after noon or night, wind energy is the promising renewable resource by excellence under the local climatic conditions of the studied region. In fact, the optimal levelized cost of energy is ranging from 0.3101 and 0.3716 € per kW h. For these cases, the load distribution profile and the storage capacity will make the difference.

Finally, the optimization methodology described in this study provides a very important systematic approach to the design, analysis and optimization of hybrid energy systems.

References

[1] Mitchell K, Nagrial M, Rizk J. Simulation and optimisation of renewable energy systems. Electr Power Energy Syst 2005;27:177–88.

[2] Elhadidy MA, Shaahid SM. Parametric study of hybrid (wind+solar+diesel) power generating systems. Renewable Energy 2000;21:129–39.

[3] Bakos GC, Tsagas NF. Techno-economic assessment of a hybrid solar/wind installation for electrical energy saving. Energy Build 2003;35:139–45.

[4] Yang H, Lu L, Zhou W. A novel optimization sizing model for hybrid solar–wind power generation system. Sol Energy 2007;81:76–84.

[5] Kellogg W, Nehrir MH, Venkataramanan G, Gerez V. Optimal unit sizing for a hybrid wind/photovoltaic generating system. Electr Power Syst Res 1996;39:35–8.

[6] Seeling-Hochmuth GC. A combined optimisation concept for the design and operation strategy of hybrid-PV energy systems. Sol Energy 1997;61:77–87.

[7] Chun-Hua Li, Zhu Xin-Jian, Cao Guang-Yi, Sui Sheng, Hu Ming-Ruo. Dynamic modeling and sizing optimization of stand-alone photovoltaic power systems using hybrid energy storage technology. Renewable Energy 2009;34:815–26.

[8] Habib⁎ MA, Said SAM, El-Hadidy MA, Al-Zaharna I. Optimization procedure of a hybrid photovoltaic wind energy system. Energy 1999;24:919–29.

[9] Rajkumar* RK, Ramachandaramurthy 1 VK, Yong 1 BL, Chia 1 DB. Techno-economical optimization of hybrid pv/wind/battery system using Neuro-Fuzzy. Energy 2011;36:5148–53.

[10] Md Darus Z, Hashim NA, Abdul Manan SN, Abdul Rahman MA, Abdul Maulud KN, Abdul Karim O. The development of hybrid integrated renewable energy system (wind and solar) for sustainable living at Perhentian Island, Malaysia. Eur J Soc Sci 2009;9:557–63.

[11] Protegeropoulos C, Brinkworth BJ, Marshall RH. Sizing and techno-economical optimization for hybrid solar photovoltaic/wind power systems with battery storage. Int J Energy Res 1997;21:465–79.

[12] Eke R, Kara O, Ulgen K. Optimization of a wind/PV hybrid power generation system. Int J Green Energy 2005;2:57–63.

[13] Borowy BS, Salameh ZM. Optimum photovoltaic array size for a hybrid wind–PV system. IEEE Trans Energy Convers 1994;9:482–8.

[14] Borowy BS, Salameh ZM. Methodology for optimally sizing the combination of a battery bank and PV array in a wind–PV hybrid system. IEEE Trans Energy Convers 1996;11:367–75.

[15] Markvart T. Sizing of hybrid photovoltaic–wind energy systems. Sol Energy 1996;57:277–81.

[16] Bagul AD, Salameh ZM, Borowy B. Sizing of a stand-alone hybrid wind–photovoltaic using a three-event probability density function. Sol Energy 1996;56:323–35.

[17] Morgan TR, Marshall RH, Brinkworth BJ. ARES—a refined simulation programme for the sizing and optimization of autonomous hybrid energy systems. Sol Energy 1997;59:205–15.

[18] Celik AN. Optimisation and techno-economic analysis of autonomous photovoltaic–wind hybrid energy systems in comparison to single photovoltaic and wind systems. Energy Convers Manage 2002;43:2453–68.

[19] Yang HX, Burnett L, Lu J. Weather data and probability analysis of hybrid photovoltaic–wind power generation systems in Hongkong. Renewable Energy 2003;28:1813–24.

[20] Tina GM, Gagliano S, Raiti S. Hybrid solar/wind power system probabilistic modelling for long term performance assessment. Sol Energy J 2006;80:578–88.

[21] Ashok S. Optimized model for community-based hybrid energy system. Renewable Energy 2007;32:1155–64.

[22] Ekren Orhan, Ekren Banu Yetkin. Size optimization of a PV/wind hybrid energy conversion system with battery storage using response surface methodology. Appl Energy 2008;85:1086–101.

[23] Kleijnen JPC. Statistical tools for simulation practitioners. 1st ed.. New York, NY: Marcel Dekker Inc; 1987.

[24] Taher Maatallah, Souheil El Alimi*, Sassi Ben Nassrallah. Performance modeling and investigation of fixed, single and dual-axis tracking photovoltaic panel in Monastir city. Renewable Sustainable Energy Rev 2011; 5:4053–66.
[25] Duffie JA, Beckman WA. Solar engineering of thermal processes. New York, NY: John Wiley and Sons; 1991.
[26] Posadillo R, López LR. Evaluation of the performance of three diffuse hourly irradiation models on tilted surfaces according to the utilizability concept. Energy Convers Manage 2009;50:2324–30.
[27] Chang TP. Output energy of a photovoltaic module mounted on a single-axis tracking system. Appl Energy 2009;86:2071–8.
[28] Díaz-Dorado E, Suarez-Garcia A, Carillo CJ, Cidràs J. Optimal distribution for photovoltaic solar trackers to minimize power losses caused by shadows. Renewable Energy 2011;36:1826–35.
[29] Berger W, Simon FG, Weimann K, Alsema EA. A novel approach for the recycling of thin film photovoltaic modules. Resour Conserv Recycl 2010;54:711–8.
[30] Syafaruddin Karatepe E, Hiyama T. Polar coordinated fuzzy controller based real-time maximum-power point control of photovoltaic system. Renewable Energy 2009;34:2597–606.
[31] Kaldellis JK. Optimum technoeconomic energy autonomous photovoltaic solution for remote consumers throughout Greece. Energy Convers Manage 2004;45:2745–60.
[32] Kim HS, Kim JK, Min BD, Yoo DW, Kim HJ. A highly efficient PV system using a series connection of DC–DC converter output with a photovoltaic panel. Renewable Energy 2009;34:2432–6.
[33] Abdolzadeh M, Ameri M. Improving the effectiveness of a photovoltaic water pumping system by spraying water over the front of photovoltaic cells. Renewable Energy 2009;34:91–6.
[34] Santamouris M, Tselepidaki I, Dris N. Evaluation of models to predict solar radiation on tilted surfaces for the Mediterranean region. Sol Wind Technol 1990;7:585–9.
[35] Li DHW, Lam JC. Predicting solar irradiance on inclined surfaces using sky radiance data. Energy Convers Manage 2004;45:1771–83.
[36] Benghanem M. Optimization of tilt angle for solar panel: case study for Madinah, Saudi Arabia. Appl Energy 2011;88:1427–33.
[37] Dorota AC. Recommendation on modeling of solar energy incident on a building envelope. Renewable Energy 2009;34:736–41.
[38] Hottel HC, Woertz BB. Performance of flat plate solar heat collectors. Trans ASME 1942;64:91.
[39] Liu BYH, Jordan RC. The long term average performance of flat-plate solar energy collectors: with design data for the US, its outlying possessions and Canada. Sol Energy 1963;7:53–74.
[40] Reindl DT, Beckman WA, Duffie JA. Diffuse fraction corrections. Sol Energy 1990;45:1–7.
[41] Perez R, Seals R, Ineichen P, Steward R, Menicucci D. A new simplified version of the Perez diffuse irradiance model for tilted surfaces. Sol Energy 1987;39:221–32.
[42] Puri VM, Jiminer R, Menzer M, Costello FA. Total and non-isotropic diffuse insolution on tilted surfaces. Sol Energy 1980;25:85–90.
[43] Klucher TM. Evaluation of models to predict insolation on tilted surfaces. Sol Energy 1979;23:111–4.
[44] Temps RC, Coulson JL. Solar radiation incident upon slopes of different orientations. Sol Energy 1977;19:179–84.
[45] Gueymard C. An anisotropic solar irradiance model for tilted surfaces and its comparison with engineering selected algorithms. Sol Energy 1987;38: 367–86.
[46] Lubitz WD. Effect of manual tilt adjustments on incident irradiance on fixed and tracking solar panels. Appl Energy 2011;88:1710–9.
[47] Chang TP. Performance evaluation for solar collectors in Taiwan. Energy 2009;34:32–40.
[48] Neville RC. Solar energy collector orientation and tracking mode. Sol Energy 1978;20:7–11.
[49] Morcos VH. Optimum tilt angle and orientation for solar collectors in Assiut, Egypt. Renewable Energy 1994;4:291–8.
[50] Al-Mohamad A. Efficiency improvements of photo-voltaic panels using a sun tracking system. Appl Energy 2004;79:345–54.
[51] Abdallah S. The effect of using sun tracking systems on the voltage–current characteristics and power generation of flat plate photovoltaics. Energy Convers Manage 2004;45:1671–9.
[52] Huang BJ, Sun FS. Feasibility study of one axis three positions tracking solar PV with low concentration ratio reflector. Energy Convers Manage 2007;48: 1273–80.
[53] Sungur C. Multi-axes sun-tracking system with PLC control for photovoltaic panels in Turkey. Renewable Energy 2009;34:1119–25.
[54] Skoplaki E, Palyvos JA. On the temperature dependence of photovoltaic module electrical performance: a review of efficiency/power correlations. Sol Energy 2009;83:614–24.
[55] Stultz JN, Wen LC Thermal performance testing and analysis of photovoltaic modules in natural sunlight. DOE/JPL LSA task report 1977:5101–5131.
[56] Kou Q, Klein SA, Beckman WA. A method for estimating the long-term performance of direct-coupled PV pumping systems. Sol Energy 1998;64: 33–40.
[57] Jamil M. Wind power statistics and evaluation of wind energy density. Wind Eng 1994;18:227–40.
[58] Freris LL. Wind energy conversion systems. 1st ed.. UK: Prentice-Hall International; 1990.
[59] Lun IYF, Lam JC. A study of Weibull parameters using long-term wind observations. Renewable Energy 2000;20:145–53.
[60] Hau E. Wind turbines. Fundamentals, technologies, application, economics. 1st ed.. Germany: Springer; 2000.
[61] Burton T, Sharpe D, Jenkins N, Bossanyi E. Wind energy handbook. 1st ed. England: John Wiley and Sons, Ltd.; 2001.
[62] Mathew S, Pandey KP, Kumar A. Analysis of wind regimes for energy estimation. Renewable Energy 2002;25:381–99.
[63] Weisser D. A wind energy analysis of Grenada: an estimation using the Weibull density function. Renewable Energy 2003;28:1803–12.
[64] Tuller SE, Brett AC. The characteristics of wind velocity that favor the fitting of a Weibull distribution in wind speed analysis. J Climate Appl Meteorol 1984;23:124–34.
[65] Carta JA, Ramirez P, Velazquez S. A review of wind speed probability distributions used in wind energy analysis case studies in the Canary Islands. Renewable Sustainable Energy Rev 2009;13:933–55.
[66] Ucar A, Balo F. Assessment of wind power potential for turbine installation in coastal areas of Turkey. Renewable Sustainable Energy Rev 2010;14:1901–12.
[67] Vogiatzis N, Kotti K, Spanomitsios S, Stoukides M. Analysis of wind potential and characteristics in North Aegean, Greece. Renewable Energy 2004;29: 1193–208.
[68] Justus CG, Amir Mikhail. Height variation of wind speed and wind distributions statistics. Geophys Res Lett 1976;3:261–4.
[69] Nfaoui H, Bahraui J, Darwish ASK, Sayigh AAM. Wind energy potential in Morocco. Renewable Energy 1991;1:1–8.
[70] Khogali A, Albar OF, Yousif B. Wind and solar energy potential in Makkah (Saudi Arabia)—comparison with Red Sea coastal sites. Renewable Energy 1991;1:435–40.
[71] Johnson GL. Wind energy systems. USA: Prentice-Hall; 1985.
[72] Kershman SA, Rheinlander J, Gabler H. Seawater reverse osmosis powered from renewable energy sources hybrid wind/photovoltaic/grid power supply for small scale desalination in Libya. Desalination 2002;153:17–23.
[73] Akgad A, Dinler A. A new method to estimate Weibull parameters for wind energy applications. Energy Convers Manage 2009;50:1761–6.
[74] Dorvlo ASS. Estimating wind speed distribution. Energy Convers Manage 2002;43:2311–8.
[75] Ucar A, Balo F. Evaluation of wind energy potential and electricity generation at six locations in Turkey. Appl Energy 2009;86:1864–72.
[76] Tar K. Some statistical characteristics of monthly average wind speed at various height. Renewable Sustainable Energy Rev 2008;12:1712–24.
[77] Seguro JV, Lambert TW. Modern estimation of the parameters of the Weibull wind speed distribution for wind energy analysis. J Wind Eng Aerodyn 2000;85:75–84.
[78] Ahmet AS, Guler O. Evaluation of wind energy investment interest and electricity generation cost analysis for Turkey. Appl Energy 2010;87:2574–80.
[79] Dahmouni AW, Ben Saleh M, Askri F, Karkeni C, Ben Nasrallah S. Wind energy in the Gulf of Tunis, Tunisia. Renewable Sustainable Energy Rev 2010;14: 1303–11.
[80] Raichle BW, Carson WR. Wind resource assessment of the Southern Appalachian Ridges in the Southeastern United States. Renewable Sustainable Energy Rev 2009;13:1104–10.
[81] Celik AN. (a) Energy output estimation for small-scale wind power generators using Weibull-representative wind data. J Wind Eng Ind Aerodyn 2003;91: 693–707.
[82] Zong Woo Geem. Size optimization for a hybrid photovoltaic–wind energy system. Electr Power Energy Syst 2012;42:448–51.
[83] Mays LW, Tung YK. Hydrosystems engineering and management. New York, NY: McGraw Hill; 1992.
[84] Geem ZW. Harmony search optimization to the pump-included water distribution network design. Civ Eng Environ Syst 2009;26:211–21.